

## Stress effects in sol-gel derived ferroelectric thin films

L. Lian and N. R. Sottos<sup>a)</sup>

*Department of Theoretical and Applied Mechanics, University of Illinois Urbana—Champaign, Urbana, Illinois 61801*

(Received 26 August 2003; accepted 19 October 2003)

Residual stress development during processing of sol-gel derived ferroelectric thin films influences electromechanical properties and performance. The present work investigates the effects of stress on field-induced polarization switching in ferroelectric  $\text{Pb}(\text{Zr}_{0.52}\text{Ti}_{0.48})\text{O}_3$  (PZT) (52/48) thin films. Film response is measured as a function of externally applied mechanical stress using a double-beam laser-Doppler heterodyne interferometer. This apparatus successfully eliminates any displacement contribution from flexural vibration of the substrate and enables measurement of the strain-electric field hysteresis loops as a function of applied stress. The field-induced strain in the PZT film increases with increasing compressive stress, while the opposite trend is observed for applied tensile stress. The dependence of electromechanical response on the external stress is attributed to the initial tensile residual stress state in the film. Tensile stress creates an in-plane clamping effect on the domains in the film, hindering polarization switching. The application of a compressive stress reduces tensile residual stress in the film and the constraint on the domains, leading to higher field-induced strains. Applied tensile stress amplifies the clamping effect, leading to lower field-induced strains. © 2004 American Institute of Physics. [DOI: 10.1063/1.1632019]

### I. INTRODUCTION

Ferroelectric thin films are used in a wide variety of applications that include microactuators, microsensors, and ultrasonic motors,<sup>1–4</sup> as well as nonvolatile computer memories and switching capacitors for integrated circuitry.<sup>5,6</sup> Among the many families of ferroelectrics, perovskite  $\text{Pb}(\text{Zr}_x\text{Ti}_{1-x})\text{O}_3$  (or PZT) thin films are the most extensively used due to their remarkable ferroelectric, piezoelectric, and pyroelectric properties, especially when the composition is near the morphotropic phase boundary ( $x \sim 0.5$ ). Ferroelectric thin films can be prepared by a number of different deposition methods which include chemical vapor deposition,<sup>7</sup> sputtering,<sup>8</sup> laser ablation,<sup>9</sup> and chemical solution methods such as sol-gel processing.<sup>10</sup> The sol-gel method is preferred for many applications because it offers both compositional control and reduced-temperature processing of highly uniform, dense, crack-free films.

Significant residual stresses develop in sol-gel processing of ferroelectric thin films during the transformation of the metalorganic gel to the metal oxide (i.e., ceramic) on heat treatment. The behavior of the film during this process can be considered in several stages: (i) drying of solvent and pyrolysis of organics, (ii) structural rearrangement and densification, (iii) crystallization, and (iv) cooling.<sup>11</sup> The total residual stress in the final polycrystalline film consists of intrinsic and extrinsic contributions. The intrinsic stress is induced by shrinkage and constrained densification during drying and firing, formation of intergranular stresses as anisotropic grains grow and by structural transformations at the Curie temperature. The intrinsic stresses due to shrinkage

depend on the relative rates of evaporation, viscous deformation and flow of liquid through the pores of the gel. Extrinsic thermal stresses are induced upon cooling due to the mismatch between the thermoelastic properties of the film with those of the substrate, while further extrinsic stress originates from the lattice parameter mismatch between the film and the substrate. Residual stresses on the order of several hundred MPa have been reported for various ferroelectric thin films.<sup>12–20</sup>

Several researchers have attributed changes in ferroelectric film structure and properties to the residual stress state. Tuttle *et al.*<sup>12</sup> reported that the sign of the film stress at the Curie point controls the orientation of the domain structure and, thus, the switchable spontaneous polarization and strain in PZT thin films. Compressive stresses upon cooling through the Curie point resulted in domains with their *c*-direction and polarization vector normal to the film surface, while tensile stresses induced domains with their *a*-direction normal to the surface and with polarization vector in the plane. As a result, PZT films deposited on sapphire under compressive residual stress exhibited superior ferroelectric properties as compared to films deposited on silicon substrates under tensile residual stress. Kweon, Yi, and Choi<sup>13</sup> also found that the *c*-axis orientation ratio was related to the intrinsic stress generated during deposition of lead titanate films.

Reduction in the residual stress state due to annealing has led to measurable changes in the poling direction and switching behavior of PZT films.<sup>14</sup> Lappalainen, Frantti, and Lantto<sup>15</sup> have also reported an increase in dielectric constant and a decrease in coercive field with decreasing residual stress for Nd-modified PZT films. Garino and Harrington<sup>16</sup> studied residual stress effects in sol-gel derived PZT films on platinumized Si wafers. Tensile residual stresses of several hun-

<sup>a)</sup> Author to whom correspondence should be addressed; electronic mail: n-sottos@uiuc.edu

dred MPa were measured. The influence of these stresses on ferroelectric properties was ascertained through electrical measurements on a film with and without the application of an external mechanical stress. Decreasing the tensile residual stress in the film by  $\sim 30\%$  was found to increase the remnant polarization by  $\sim 11\%$  and the dielectric constant by  $\sim 2\%$ .

More recently, Lian and Sottos<sup>21</sup> reported significant changes in the properties of PZT thin films with different thickness and crystallographic texture. The measured piezoelectric constants, field-induced strains, and dielectric constants all decreased with diminishing film thickness. In addition, films with (100) preferred orientation had higher piezoelectric coefficients, smaller loss factors, and higher saturation and remnant polarizations than films with (111) preferred orientation. The thickness and texture dependence of the electromechanical properties was attributed to the residual stress state in the film, which is also dependent on thickness and processing conditions.

Analytical models developed for epitaxial ferroelectric thin films predict dramatic changes in the dielectric, piezoelectric, and pyroelectric constants with the application of external stress.<sup>22–24</sup> Moreover, the theory developed by Emelyanov, Pertsev, and Kholkin<sup>22</sup> indicates that mechanical loading of epitaxial films can be employed for fine tuning of their ferroelectric properties. Although these models and mechanisms are not applicable to polycrystalline ferroelectric films, the predicted stress effects are interesting.

In bulk ferroelectric ceramics, applied compressive stress is known to have a significant effect on electromechanical behavior. Cao and Evans<sup>25</sup> investigated the stress-induced depolarization in poled hard and soft PZT. The strain and depolarization were measured continuously while uniaxial compressive stress was applied either parallel or perpendicular to the poling direction of a compression cuboid. Both materials were nonlinear when the stress in the poling direction exceeded  $\sim 20$  MPa, and exhibited permanent deformations ( $\sim 0.5\%$ ) and residual depolarization ( $\sim 80\%$ ) after exposure to stresses above 500 MPa. Lynch<sup>26,27</sup> measured strain-electric field and polarization-electric field hysteresis loops of lead lanthanum zirconate titanate (PLZT) and PZT at various compressive stress levels. Both the field-induced strain and field-induced polarization decreased significantly as the compressive stress parallel to the electric field was increased. The significant effects of applied stress observed in bulk ferroelectric ceramics provide further support for stress-dependent behavior in ferroelectric thin films under high levels of residual stress.

The present work investigates the influence of applied stress on field-induced polarization switching in ferroelectric PZT (52/48)  $[\text{Pb}(\text{Zr}_{0.52}\text{Ti}_{0.48})\text{O}_3]$  thin films. The field-induced strain in the film is measured using laser interferometry while an external stress is applied by bending the substrate.

## II. STRESS EFFECT ON FIELD-INDUCED BEAM DEFLECTION

Measuring the effect of stress on the field-induced strain in a ferroelectric thin film is challenging due to the planar

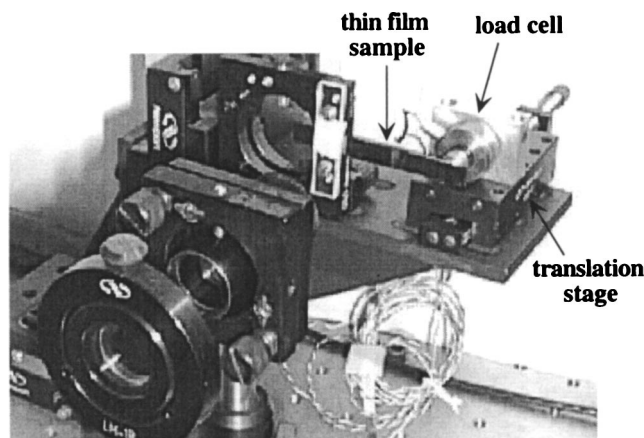


FIG. 1. Experimental apparatus for applying bending loads to thin-film ferroelectric samples during interferometric measurements.

geometry and small out-of-plane displacements. Traditional piezoelectric measurement techniques such as the resonance method and the strain gauge method used for bulk ferroelectrics are not suitable for films. In addition, the experimental setup must allow for the application of an external stress and direct measurement of the deformation of the film. Several high-resolution interferometric techniques have been adopted for characterizing thin-film response. Li *et al.*<sup>28–30</sup> constructed a single-beam Michelson interferometer to study the electromechanical coupling of a variety of ferroelectric thin films over a wide range of frequencies. Kholkin *et al.*<sup>31</sup> and more recently Gerber *et al.*<sup>32</sup> and Fernandes *et al.*<sup>33</sup> used a modified Mach–Zehnder interferometer to investigate the electric field, frequency, and time-dependent piezoelectric response of PZT thin films. While Michelson and Mach–Zehnder interferometers have high resolutions, both are sensitive to the surrounding environment and require significant effort to align the laser beams and stabilize the working point. Lian and Sottos<sup>21</sup> developed a robust, laser-Doppler heterodyne interferometric technique to quantify changes in the  $d_{33}$  piezoelectric coefficients and field-induced strains of rigidly mounted PZT thin films. This single beam interferometric method was used initially in the current study to measure field-induced displacements in films subjected to applied stress.

## A. Materials and experimental procedure

PZT thin film samples were obtained from NZ Applied Technologies (Wolburn, MA) with a Zr/Ti ratio of 52/48. The films were deposited on platinumized silicon wafer substrates using the sol-gel technique and cut into rectangular beams. The crystallization behavior of these films was examined at room temperature by x-ray diffraction and the microstructure was evaluated by scanning electron microscopy.<sup>21</sup> Films tested in the current study had well aligned columnar grains with a preferred (100) orientation and a thickness of  $1.6 \mu\text{m}$ . The width, length, and thickness of the beam were 9, 60, and 0.38 mm, respectively.

Stress effects were investigated by applying a static bending load to the film and substrate using the apparatus shown in Fig. 1. One end of the beam sample was clamped

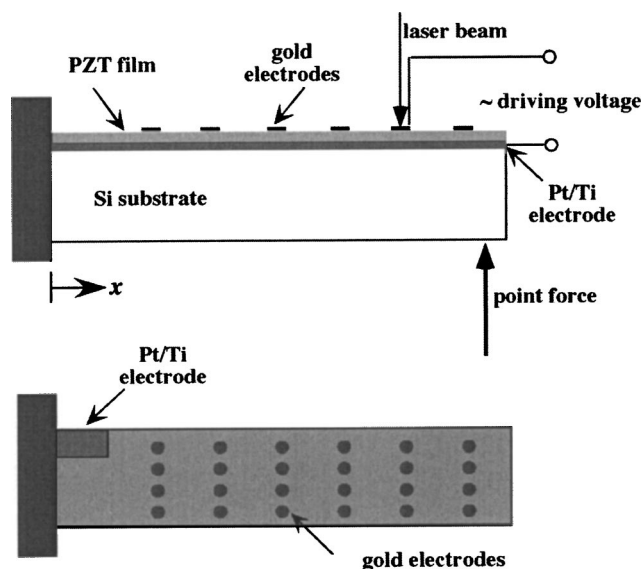


FIG. 2. Schematic of the beam sample used in the interferometric measurements.

onto a mirror mount that could be manually adjusted for angular tilt when aligning the interferometer. A load cell (Sensotec, Model 31/1426-03) attached to a translation stage, which moved perpendicularly with respect to the sample surface, measured force applied at the free end of the cantilever beam. The position of the translation stage controlled the amount of applied force. A high performance process indicator (OMEGA, Model DP41S) supplied the excitation voltage to the load cell and displayed the output from it.

Initially, the single-beam laser-Doppler heterodyne interferometer described in Lian and Sottos<sup>21</sup> was used to measure the deflection of the entire beam sample under different compressive stress levels. A schematic of a typical beam sample as prepared for the interferometric measurements is shown in Fig. 2. Gold electrodes of 1 mm in diameter were evaporation deposited onto the top surface of the PZT film through a shadow mask. A portion of the PZT film at the corner of the sample was etched away to leave the Pt layer exposed for the bottom electrode. Electric contacts were made to the top and bottom electrodes with fine copper wires of 25.4  $\mu\text{m}$  in diameter. Prior to any interferometric measurements, a static point force was applied at the end of the cantilever beam sample by adjusting the position of the translation stage. The stress in the PZT film due to bending of the substrate was calculated from the measured force using beam theory. The interferometer was then carefully aligned in the center of a single top electrode. The portion of the unpoled film between the selected top electrode and bottom electrode was driven by a large sinusoidal 1.0 kHz ac electric field. During the experiment, the sample was translated horizontally at a speed of 5  $\mu\text{m}/\text{s}$  while the lock-in amplifier recorded amplitude of the out-of-plane velocity at each point on the scan across the film surface. After recording the data, the magnitude of the static point force was incremented and the interferometric measurement repeated.

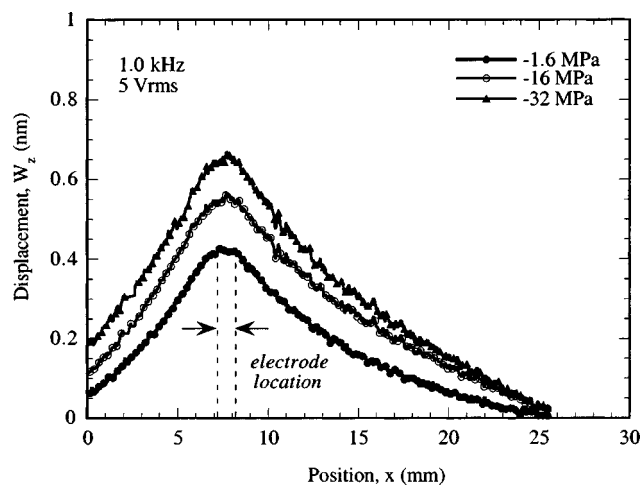


FIG. 3. Out-of-plane displacement profile of a PZT/Si cantilever beam at different applied compressive stress levels.

## B. Results

A plot of the beam displacement as a function of applied load is shown in Fig. 3. A significant increase in displacement due to excitation of the film occurs for increasing values of applied compressive stress. The measured beam displacements in Fig. 3 are large in comparison to the film displacements reported previously by Lian and Sottos.<sup>21</sup> The cantilever mounting method enables the application of an external load to the film, however, it also allows flexural deflection of the substrate when the ferroelectric film is activated. Without a rigid back mount, the entire length of the beam is excited by the small portion of the film under the electrode. Hence, the profiles reported in Fig. 3 are a combination of both film and substrate displacement. Nevertheless, the vibration of the beam is due solely to the deformation of the film induced by applied electric field and the change in the displacement profiles in Fig. 3 indicate that the response of the film depends significantly on the applied stress.

Although the residual stress was not measured directly for the films in the current investigation, previously reported stress data for PZT films deposited on platinized Si substrates<sup>12,14,16,18</sup> provide sufficient evidence that these films are in a state of residual tension. The residual stress state in the films is biaxial, but the application of biaxial stress is prohibitive due to the beam-like sample geometry. As a result, only the residual stress in the longitudinal direction of the beam is relieved or intensified during the bending experiment. The increased displacement response with the application of compressive stress in Fig. 3 is attributed to the relief of residual tensile stress in the film.

## III. STRESS EFFECTS ON FIELD-INDUCED FILM STRAIN

### A. Double-beam heterodyne interferometer

In order to explicitly investigate stress effects on film response, we needed to eliminate the deflection of the substrate from the experimental measurements. A double-beam interferometer in which the probing beam reflects from both the front and back surfaces of the sample (Fig. 4) was con-

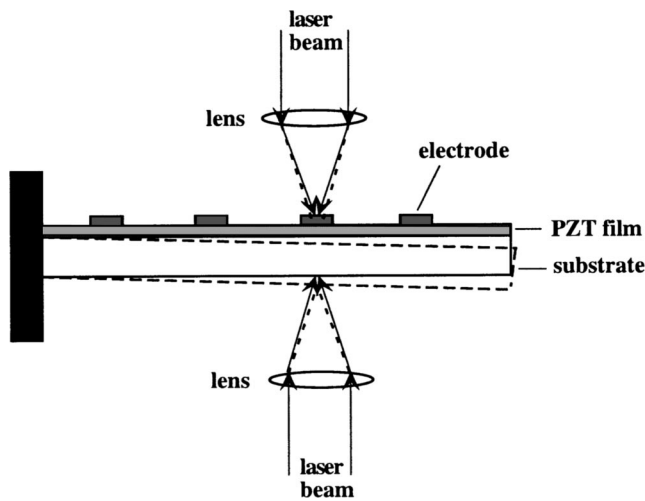


FIG. 4. Schematic of a sample in the double-beam interferometer.

structed by modifying the single-beam heterodyne interferometer configuration reported in Lian and Sottos.<sup>21</sup> The bending contribution of the substrate is removed by the exact cancellation of the optical path length change of the two beams impinging on the sample. Use of a double-beam interferometer for strain measurements in bulk ferroelectric materials was described by Zhang, Jang, and Cross<sup>34</sup> and later applied to characterization of ferroelectric thin films.<sup>31–33</sup>

The full optical arrangement of the double-beam Doppler heterodyne interferometer is shown in Fig. 5. A single frequency, linearly polarized laser beam of wavelength 514.5 nm from an argon laser (Lexel Laser model 3500) is incident upon a 40 MHz acousto-optic modulator (AOM) producing two beams which are sent along different arms of the inter-

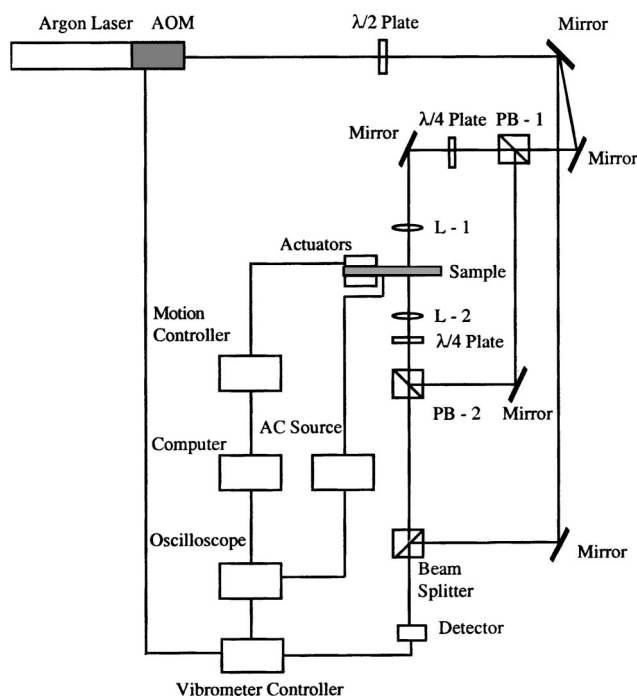


FIG. 5. Double-beam laser-Doppler heterodyne interferometer.

ferometer. One beam is shifted in frequency by 40 MHz and used as a reference beam. The other beam, which has the same frequency as the beam incident upon the AOM, is directed to the backside of the substrate first and then reflected to the front surface of the film and sharply focused at normal incidence onto a point just opposite to the probing point on the other side. The  $\lambda/2$  plate is used to rotate the polarization vectors of the sample and reference beams to the horizontal direction. The combination of the polarizing beam splitters and the quarter-wave plates in the probing arm of the interferometer reduces the light loss of the sample beam. The convex lenses L-1 and L-2 have the same focal lengths. They are mounted onto translation stages and their positions are carefully adjusted so that the reflecting surfaces of the sample are exactly in the focal planes of the lenses.

The laser beams impinging on the back and front surfaces of the sample needed to be colinear to completely eliminate the substrate bending effect. By placing a partial reflective mirror in the position of the sample and then carefully adjusting the tilt angle and position of the polarized beam splitter (PB-2) and lens (L-2), the laser beams passing through and reflected back from the partial reflective mirror were aligned on top of each other. The reference and sample beams were recombined at the nonpolarizing beam splitter. The resulting interference pattern at the surface of the photodetector produced a voltage proportional to the intensity of light focused on it. The frequency of the interference signal received by the photodetector was equal to 40 MHz plus or minus the instantaneous Doppler frequency shift. The principle of operation and instrumentation of this double-beam interferometer is the same as that described in Lian and Sottos<sup>21</sup> for the single-beam Doppler heterodyne interferometer except that an oscilloscope (Tektronix, TDS 420) was used instead of the lock-in amplifier to measure the transient field-induced strains in the PZT film.

As for the single-beam interferometric measurements, a static point force was first applied to the end of the cantilever beam sample by adjusting the position of the translation stage. The double-beam interferometer was carefully aligned so that sample beam was focused onto the center of a single top electrode. The portion of the unpoled film between the bottom and top electrode was then driven by a large sinusoidal 1.0 kHz ac electric field. An averaging function of the digital oscilloscope was used to acquire the signal from the vibrometer controller. The time-dependent out-of-plane deformation of the film was obtained by integrating the output signal of the oscilloscope with respect to time. After the data was recorded, the magnitude of the static point force was changed and the interferometric measurement was repeated at the same point on the film surface.

## B. Results and discussion

The displacement profile in the vicinity of the activated top electrode was measured first with no applied stress to ensure the bending contribution of the substrate was completely eliminated. The amplitude and frequency of the driving voltage applied were 20 V (peak to peak) and 1.0 kHz, respectively. The displacement quickly diminished outside

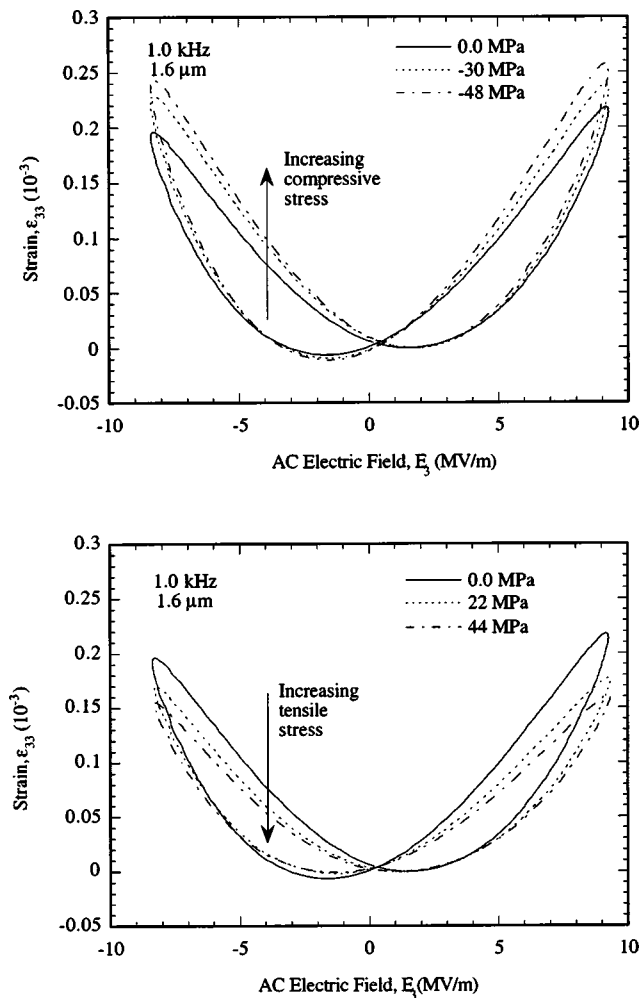


FIG. 6. Field-induced strains in 1.6- $\mu\text{m}$ -thick PZT (52/48) film under: (a) increasing compressive bending load; (b) increasing tensile bending load.

the electroded areas indicating that the bending contribution of the substrate was successfully subtracted from the measurement by using the double-beam interferometric technique.

Typical butterfly-type strain hysteresis loops are shown in Fig. 6(a) for the PZT film under increasing compressive bending load. Each loop represents an average of 10 000 cycles. As the external compressive stress in the film increased from zero to 48 MPa, the field-induced strain increased about 18%. In addition, strain hysteresis loops were measured for the PZT film under increasing tensile bending load [Fig. 6(b)]. As the external tensile stress in the film increased from zero to 44 MPa, the field-induced strain decreased about 26%.

Results of these bending experiments indicate that the initial tensile residual stress state in the films creates an in-plane clamping effect on the domains. The application of a compressive stress relieves the tensile residual stress in the film and the constraint on the domains, which leads to higher field-induced strains [Fig. 6(a)]. On the other hand, the application of tensile stress amplifies the clamping effect, which leads to decreased field-induced strains in the film as the external stress increases [Fig. 6(b)]. The changes in field-induced strains with applied stress reported in Fig. 6 are

consistent with previous measurements of stress effects on remnant polarization and dielectric constant.<sup>20</sup>

Residual stress effects appear to play a critical role in determining the properties and performance of ferroelectric thin-film structures. These effects will become even more dominant as the characteristic length scale of film devices becomes smaller and smaller. Ong<sup>18</sup> recently reported that the residual stress in PZT films processed by the sol-gel technique increases significantly with diminishing film thickness. Changes in the residual stress state with film thickness are likely to be the primary cause of the dramatic decrease in field-induced strains with decreasing film thickness measured by Lian and Sottos.<sup>21</sup> Understanding the effects of residual stresses developed during processing on film properties and how to tailor these stresses for optimal device performance is essential to advance this technology for the next generation of electromechanical devices.

#### IV. CONCLUSIONS

PZT (52/48) film response was measured as a function of externally applied mechanical stress using laser-Doppler heterodyne interferometry. Mechanical stress was applied by static beam bending, and the displacement profile of the film/substrate beam was measured with a single-beam interferometer. The displacement of the beam was found to increase as the applied uniaxial compressive stress in the PZT film increased. The electric field response of the film was successfully isolated from the vibration of the substrate by using a double-beam laser-Doppler interferometer. Application of a compressive bending stress to relieve the tensile residual stress in PZT (52/48) film increased the field-induced strains. The opposite effect was observed for application of a tensile stress. These results indicate that the initial residual stress state in the film has a significant influence on electromechanical performance of the film.

#### ACKNOWLEDGMENTS

This work was supported by the National Science Foundation under grant No. NSF CMS 00-88206. The authors would like to acknowledge helpful conversations with Professor David Payne and Ryan Ong in the Department of Material Science and Engineering at the University of Illinois at Urbana-Champaign.

- <sup>1</sup>E. S. Kim and R. S. Muller, *IEEE Electron Device Lett.* **EDL-7**, 254 (1987).
- <sup>2</sup>S. W. Wenzel and R. M. White, *IEEE Trans. Electron Devices* **ED-35**, 735 (1988).
- <sup>3</sup>D. L. Polla, R. S. Muller, and R. M. White, *IEEE Electron Device Lett.* **EDL-7**, 254 (1986).
- <sup>4</sup>R. M. Morney, R. M. White, and R. T. Howe, *Proceedings of the IEEE Ultrasonics Symposium, Montreal, 3–6 October, 1989*, p. 745.
- <sup>5</sup>D. Bondurant and F. Gnadinger, *IEEE Spectrum* **26**, 30 (1989).
- <sup>6</sup>M. H. Frey and D. A. Payne, *Appl. Phys. Lett.* **63**, 2753 (1993).
- <sup>7</sup>T. Nakagawa, J. Yamaguchi, M. Okugama, and Y. Hamakawa, *Jpn. J. Appl. Phys., Part 2* **21**, 655 (1982).
- <sup>8</sup>Z. Surowiak, H. Zajosz, and R. Dytry, *Thin Solid Films* **51**, 359 (1978).
- <sup>9</sup>H. Kidoh, T. Ogawa, H. Yashima, A. Morimoto, and T. Shimizu, *Jpn. J. Appl. Phys., Part 1* **30**, 2167 (1991).
- <sup>10</sup>K. D. Budd, S. K. Dey, and D. A. Payne, *Br. Ceram. Proc.* **36**, 107 (1985).
- <sup>11</sup>C. D. E. Lakeman, Z. Xu, and D. A. Payne, *J. Mater. Res.* **10**, 2042 (1995).
- <sup>12</sup>B. A. Tuttle, J. A. Voigt, T. J. Garino, D. C. Goodnow, R. W. Schwartz, D.

- L. Lamppa, T. J. Headley, and M. O. Eatough, Proceedings of the Eighth IEEE International Symposium on Applications of Ferroelectrics, New York, 30 August–2 September, 1992, pp. 344–348.
- <sup>13</sup>S. Y. Kweon, S. H. Yi, and S. K. Choi, *J. Vac. Sci. Technol. A* **15**, 57 (1997).
- <sup>14</sup>G. A. C. M. Spierings, G. J. M. Dormans, W. G. J. Moors, and M. J. E. Ulenaers, *J. Appl. Phys.* **78**, 1926 (1995).
- <sup>15</sup>J. Lappalainen, J. Frantti, and V. Lantto, *J. Appl. Phys.* **82**, 3469 (1997).
- <sup>16</sup>T. J. Garino and H. M. Harrington, *Mater. Res. Soc. Symp. Proc.* **243**, 341 (1992).
- <sup>17</sup>S. S. Sengupta, S. M. Park, D. A. Payne, and L. H. Allen, *J. Appl. Phys.* **83**, 2291 (1998).
- <sup>18</sup>R. Ong, Masters thesis, Department of Materials Science and Engineering, University of Illinois, Urbana, IL, 2001.
- <sup>19</sup>K. Yao, S. Yu, and F. E. Tay, *Appl. Phys. Lett.* **82**, 4540 (1993).
- <sup>20</sup>L. L. Zhang, J. Tsaur, and R. Maeda, *Jpn. J. Appl. Phys., Part 1* **42**, 1386 (2003).
- <sup>21</sup>L. Lian and N. R. Sottos, *J. Appl. Phys.* **87**, 3941 (2000).
- <sup>22</sup>A. Y. Emelyanov, N. A. Pertsev, and A. L. Kholkin, *Phys. Rev. B* **66**, 214108 (2002).
- <sup>23</sup>H. X. Cao, Y. Z. Wu, W. Dong, and Z. Y. Li, *Phys. Status Solidi B* **238**, 213 (2003).
- <sup>24</sup>L. Lahoche, V. Lorman, S. B. Rochal, and J. M. Roelandt, *J. Appl. Phys.* **91**, 4973 (2002).
- <sup>25</sup>H. Cao and A. G. Evans, *J. Am. Ceram. Soc.* **76**, 890 (1993).
- <sup>26</sup>C. S. Lynch, *J. Intell. Mater. Syst. Struct.* **9**, 555 (1998).
- <sup>27</sup>C. S. Lynch, *Acta Mater.* **44**, 4137 (1996).
- <sup>28</sup>J.-F. Li, D. D. Viehland, T. Tani, C. D. E. Lakeman, and D. A. Payne, *J. Appl. Phys.* **75**, 442 (1994).
- <sup>29</sup>J.-F. Li, D. D. Viehland, T. Tani, C. D. E. Lakeman, and D. A. Payne, *J. Mater. Res.* **10**, 1435 (1995).
- <sup>30</sup>J.-F. Li and D. D. Viehland, *J. Appl. Phys.* **80**, 3451 (1996).
- <sup>31</sup>A. Kholkin, C. Wüthrich, D. V. Taylor, and N. Setter, *Rev. Sci. Instrum.* **67**, 1935 (1996).
- <sup>32</sup>P. Gerber, A. Roelofs, O. Lohse, C. Kügeler, S. Tiedke, and R. Waser, *Rev. Sci. Instrum.* **74**, 2613 (2003).
- <sup>33</sup>J. R. Fernandes, F. A. de Sa, J. L. Santos, and E. Joanni, *Rev. Sci. Instrum.* **73**, 2073 (2002).
- <sup>34</sup>Q. M. Zhang, S. J. Jang, and L. E. Cross, *J. Appl. Phys.* **65**, 2807 (1989).